A Spoof Surface Plasmon Polaritons Filter with Controllable Negative Slope Equalization Based on Surface Resistance

Chenhao Wang[1], Junjie Dong[1], Xiaomin Shi[2], and Hailong Yang[3]

[1]Xi'an Key Laboratory of Intelligence
Xi'an Technological University, Xi'an 710021, China
wangchenhao@xatu.edu.cn, xxhrlle@163.com

[2]Department of Communication Engineering
Xi'an Shiyou University, Xi'an 710065, China
xmshi@xsyu.edu.cn

[3]School of Electronic Engineering
Xi'an University of Posts and Telecommunications, Xi'an 710100, China
yanghl68@163.com

Abstract – This paper presents a novel spoof surface plasmon polariton (SSPP) filter integrated with controllable negative slope equalization. Different from traditional microwave filters, two microwave functions - amplitude compensation and interference suppression - are integrated into one device by depositing a lossy indium tin oxide (ITO) film on the rectangular corrugated stub of the SSPP unit. The key point of negative slope equalization benefits from the surface resistance of the ITO film, and the circuit model and behavior are analyzed in detail. Based on the principle, a prototype of a SSPP filter operating from S to C band is designed and fabricated. The measurement results show that the attenuation in the passband increases almost linearly from 3.5 GHz (−4.8 dB) to 6.9 GHz (−15.4 dB), indicating that −10.6 dB equalization is achieved. The improved S_{21} is attributed to the good impedance matching by sputtering the ITO film on the rectangular metal strip rather than the central strip. Due to the natural low-pass property of SSPPs, the high-order parasitic band is suppressed above the cut-off frequency of 8.5 GHz. The analyses, simulations and measurements show that the proposed SSPP filter is provided with an additional ability to compensate for positive amplitude fluctuation in wideband antennas.

Index Terms – equalization, indium tin oxide, low-pass filter, spoof surface plasmon polaritons.

I. INTRODUCTION

The amplitude compensation of frequency domain is a perpetual topic in microwave wideband systems. Although most microwave systems experience a negative slope response, where the gain decreases with increasing frequency, positive slope response is common due to chip process or device characteristics. For example, the radiation efficiency of the high-frequency band of a wideband antenna is higher than that of the low-frequency band, which requires a negative slope equalizer to smooth fluctuations.

In recent years, various types of equalizers have been proposed to smooth the system gain curves [1–5]. In [1], a substrate-integrated-waveguide (SIW) equalizer operating in millimeter wave is investigated by spraying tantalum nitride on the substrate. The positive slope transmission curves with different equalizing values of 2.8, 5.6 and 9 dB are synthesized over the whole Ka band. In [2], a gain equalizer based on periodic spiral-shaped defected ground structure is proposed, which achieved good isolation effects due to the confinement of the electric field by the grounded coplanar waveguide. Further, in order to regulate attenuation, micro-electro-mechanical system (MEMS) switches are used to achieve a reconfigurable microwave equalizer, realizing four different attenuations of 7.0, 6.6, 5.9 and 5.6 dB [3]. A number of other different equalizing structures, such as active SiGe heterojunction bipolar transistor [4] or stepped impedance resonator [5], have enabled the realization of various equalizing curves. However, due to the inherent resonance structure, the high-order periodic response of the existing microwave equalizer will deteriorate the suppression performance out of the passband of broadband systems, which is imperceptible. Additional measures need to be studied to alleviate this situation.

Spoof surface plasmon polaritons (SSPPs) are a highly confined surface mode at the interface between a dielectric and periodic metal structure, which has

Submitted On: November 23, 2023
Accepted On: August 12, 2024

https://doi.org/10.13052/2024.ACES.J.390608

attracted extensive attention. Since Pendry theoretically proved the existence of SSPPs [6] in 2004 and Hibbins experimentally confirmed the surface mode [7] in 2005, many investigations have been conducted on microwave devices based on SSPPs, such as filter [8], antenna [9] and power divider [10]. Due to inherent dispersion, surface waves higher than the asymptotic frequency cannot propagate in SSPPs, that is, the natural low-pass filter. Although the insertion loss of SSPPs is larger than other transmission structures, it provides a method to suppress the periodic response of microwave devices.

In view of the above two key points, this paper presents a novel SSPP filter with controllable negative slope equalization. The equalization and low-pass properties are explained in detail. To validate the method, a prototype is designed, simulated and measured. The results show that the proposed SSPP filter achieves a linear equalization from 3.5 GHz to 6.9 GHz with −10.6 dB equalizing value. Periodic response does not occur in the upper stopband from 8.5 GHz to 15 GHz. Compared with existing SSPP filters, the proposed filter has obvious advantages in realizing equalization and filtering functions simultaneously, which can smooth the positive slope gain response caused by higher radiation efficiency in the high-frequency band, such as wideband antennas.

II. CIRCUIT MODEL OF THE UNIT CELL

The SSPPs unit cell of the proposed filter is shown in Fig. 1 (a). The double-sided corrugated strip is coated on the transparent polyethylene terephthalate (PET) film, with relative dielectric constant $\varepsilon_r = 3$ and thickness t = 100 μm. In contrast to regular SSPP unit cells, indium tin oxide (ITO) conductive material is uniformly sputtered on the rectangular corrugated strip instead of ideal metal thin layer, as indicated by the gray region in Fig. 1 (a). The residual center metal strip is shown by the yellow region. The main parameters of the unit cell during the analysis are set as follows: the width and length of the ITO strip are h=26 mm, b=1.5 mm; the width and length of the metal strip are w=1.4 mm, l=3 mm; and the period of the unit cell is p=6 mm, respectively.

The equalization and filtering properties can be analyzed by the equivalent model of the SSPP unit cell. Since the unit cell in Fig. 1 (a) is a single conductor structure, the ground plane can be defined at infinity, that is, the RLC network as depicted in Fig. 1 (b) can be extracted and calculated using the method provided in [11]. It should be noted that the equivalent resistance R_s depends on the surface impedance Z_s of the ITO film, which can be calculated by (1):

$$\mathrm{R_s} = \frac{\mathrm{Z_s(h/2)}}{\mathrm{b}}. \tag{1}$$

Combining the structure parameters mentioned above with the setting of Z_S=2.5 Ω/□, each element is calculated as L_m=3.44 nH, L_s=0.58 nH, L_i=0.04 nH,

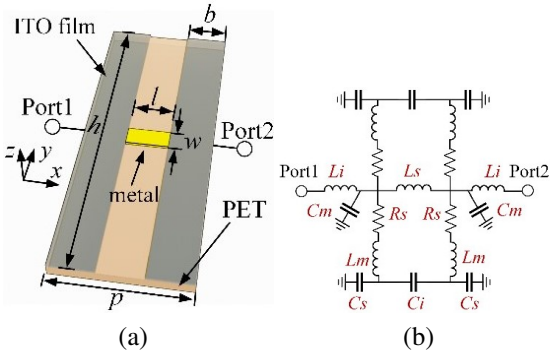

Fig. 1. Layout (a) and equivalent circuit (b) of the SSPP unit cell.

C_s=540 fF, C_m=258 fF, C_i=77 fF and R_s=20 Ω. When the surface transverse magnetic (TM) energy flows across a period length p of the unit cell, the phase and amplitude of the propagating surface wave increases and decays by a constant, respectively, which can be defined in the ABCD matrix as follows:

$$\begin{bmatrix} V_n \\ I_n \end{bmatrix} = [\mathrm{A}_M] \begin{bmatrix} V_{n-1} \\ I_{n-1} \end{bmatrix} = \begin{bmatrix} e^{\gamma_x p} V_{n-1} \\ e^{\gamma_x p} I_{n-1} \end{bmatrix}, \tag{2}$$

where $[\mathrm{V_n}, \mathrm{I_n}]$ and $[\mathrm{V_{n-1}}, \mathrm{I_{n-1}}]$ are the voltage-current pairs on both sides of the unit cell, $\gamma_x = \alpha_x + i\beta_x$ is the propagation constant in the x-direction of surface wave propagation, with α_x being the attenuation constant and β_x the phase constant. $[\mathrm{A_M}]$ is the transmission matrix of the RLC-network in Fig. 1 (b), which can be expressed in terms of R_s, L_i, L_s, L_m, C_i, C_s and C_m. For a symmetric network, the elements A, B, C and D in matrix $[\mathrm{A_M}]$ satisfy $A{\cdot}D - B{\cdot}C = 1$, hence, $\gamma_x$can be expressed as:

$$\gamma_x = \alpha_x + i\beta_x = \frac{\mathrm{arcosh(A)}}{\mathrm{p}}. \tag{3}$$

The real-part α_x and imaginary-part β_x in (3) describe the equalization and dispersion properties of the unit cell, respectively. For ease of understanding, Fig. 2 depicts the two characteristic curves. In Fig. 2 (a), similar to the lossless SSPPs, all dispersion curves obviously deviate from the light as β_x gradually increases. As the width of ITO strip h gradually decreases from 26 mm to 14 mm, the asymptotic frequency of the proposed unit cell increases from 3.5 GHz to 6.9 GHz, indicating that dispersion ability is maintained even though the ITO film is loaded and the transmission of the confined TM surface is still supported. In Fig. 2 (b), the curve of attenuation constant α_x exhibits an additional energy fading of the unit cell along with the frequency, which is manifested by the increase in the modulus of α_x. The equalization band is defined as the corresponding frequency when α_x is between a certain value and 0. For ease of understanding, an example of $\alpha_x = 26$ is provided for illustration in Fig. 2 (b). The equalization bands of the three curves start from direct current ($\alpha_x = 0$) and end

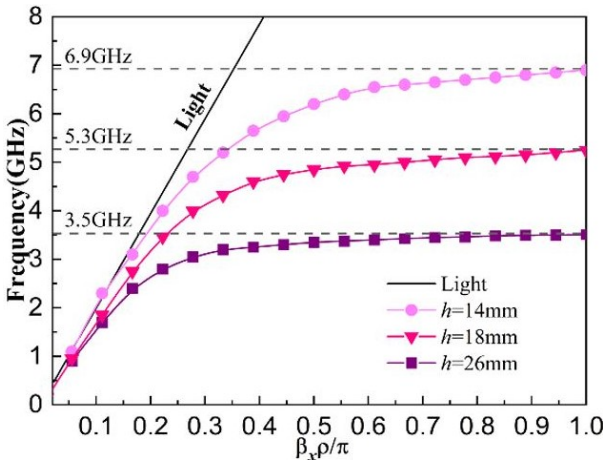

(a)

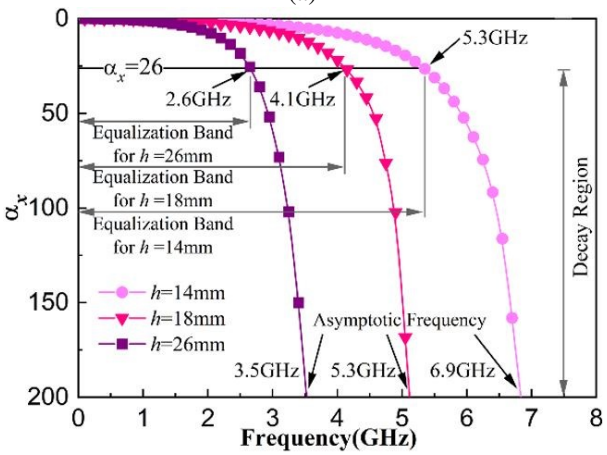

(b)

Fig. 2. Dispersion curves (a) and attenuation curves (b) of the SSPP unit cell with various widths h.

at 2.6 GHz, 4.1 GHz and 5.3 GHz ($\alpha_x = 26$) with the almost linear negative decay slopes of −9.7 Np/GHz, −6.5 Np/GHz and −5.0 Np/GHz, respectively. By converting the unit of voltage attenuation multiple to logarithm, an equalizing value of −1.35 dB can be achieved within the period length p=6 mm of a unit cell to compensate for the positive amplitude fluctuations. In addition, it can be observed that all curves converge to the constant $\alpha_x = 26$ near each asymptotic frequency. This is important because it provides an effective mean for tuning the bandwidth of the filter while maintaining a fixed equalizing value.

Furthermore, in order to investigate how well the controllable equalization of the SSPP unit cell meets different compensation requirements, the equalizing curves with various values of R_s under a fixed h=18 mm are shown in Fig. 3. All curves terminate at the same asymptotic frequency of 5.3 GHz. With R_s increasing from 5 Ω to 40 Ω, the equalizing values increase slowly, resulting in the slopes of −1.40 Np/GHz, −2.72 Np/GHz, −4.84 Np/GHz and −6.83 Np/GHz in the equalization band from 0.4 GHz to 4.0 GHz, respectively. The slope is linearly proportional to R_s, namely, the controllable amplitude compensation is achieved by the surface impedance of the ITO film. Especially when R_s decreases to 0 Ω, the ITO thin film strip degenerates into an ideal conductor, and the attenuation curve of R_s=0 Ω returns to the traditional lossless SSPPs as shown in Fig. 3, with the equalization ability no longer provided.

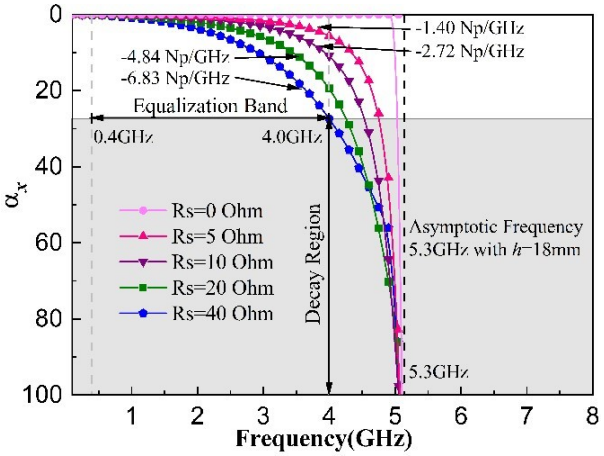

Fig. 3. Attenuation curves of the SSPP unit cell with various surface impedance Z_s.

III. THE DESIGN AND MEASUREMENT OF THE SSPP FILTER

Based on the analysis described above, a SSPP filter with controllable negative slope equalization is proposed. Figure 4 exhibits the geometry of the filter which consists of three regions: (1) coplanar waveguide (CPW) region, (2) transition region and (3) SSPP waveguide region. The geometric parameters are set as: p=6 mm, w=1.4 mm, l=3 mm, h=14 mm, d=1.2 mm and Z_S=5 Ω/□. The CPW transmission line supports transverse electro-magnetic (TEM) mode and provides 50 Ω connection node for external systems. The conversion

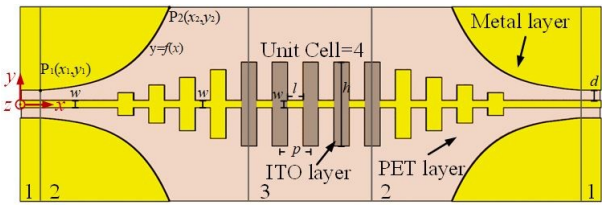

Fig. 4. Geometric configuration of the proposed SSPP unit cell consists of three regions: (1) coplanar waveguide region, (2) transition region and (3) SSPP waveguide region.

structure is used to complete smooth momentum and impedance conversion between TEM and TM mode [12]. As shown in Fig. 4, the conversion structure includes flared ground and gradient grooves, increasing the groove width from w=1.4 mm to h=14 mm in increments of 2.52 mm, and the outline of the flared ground is characterized as:

$$y = f(x) = C_1 e^{ax} + C_2, \tag{4}$$

where $x_1 \le x \le x_2$, $P_1(x_1, y_1)$ and $P_2(x_2, y_2)$ are the origin and destination of the outline, $C_1 = \frac{y_2 - y_1}{e^{ax_2} - e^{ax_1}}$, $C_2 = \frac{y_1 e^{ax_2} - y_2 e^{ax_1}}{e^{ax_2} - e^{ax_1}}$, the optimal values are a=0.14, $|x_2 - x_1| = 25\ mm$,$|y_2 - y_1| = 16.05\ mm$.

The SSPP waveguide region mainly determines the performance of the filter. As shown in Fig. 5 (a), the frequency characteristic of the SSPP filter depends on the width of the ITO strip. As h increases from 11 mm to 16 mm, the cut-off frequency decreases from 8.1 GHz to 5.3 GHz with the −10 dB equalizing bandwidth of 4.9 GHz, 2.9 GHz and 1.7 GHz, respectively. Due to the SSPP filter being a single conductor structure, the insertion loss below 3.6 GHz is relatively large, which can be improved by employing grounded SSPPs. According to the analysis in Section II, the adjustment of the equalizing value in the passband can be realized by regulating the surface resistance Z_s of the ITO film. Figure 5 (b) depicts the relationship between Z_s and the transmission curve with h=14 mm. As expected, the equalizing values within the equalization band from 3.5 GHz to 6 GHz are 8 dB, 11.5 dB, 13.6 dB and 15.6 dB, respectively, along with Z_s increases from 5 Ω to 10 Ω, 15 Ω and 20 Ω. The higher the surface resistance, the greater the response that can be compensated. These adjustable parameters provide sufficient flexibility in practical negative response, which can be applied in microwave systems with positive fluctuations such as wideband antennas.

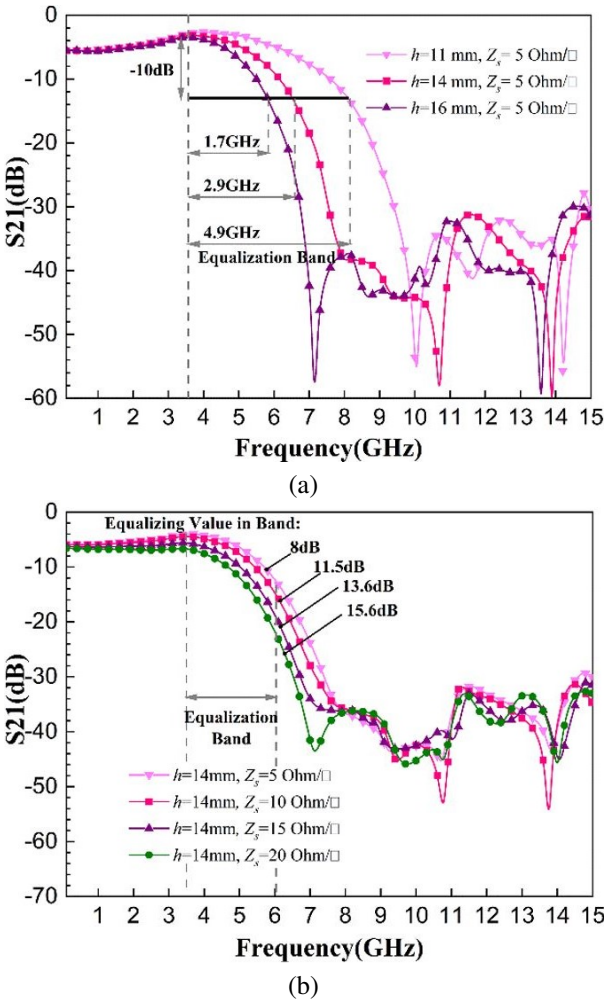

Fig. 5. (a) h-dependency of S_{21} curves and (b) Z_s-dependency of S_{21} curves.

To validate the above analysis, a prototype of the proposed SSPP filter with controllable negative slope equalization is manufactured. The flexible PET film is selected as the substrate with relative dielectric constant ε_r= 3 and layer thickness t = 100 μm. Figure 6 shows the vertical view and measurement results of the filter. The dimensions mentioned in Fig. 4 are optimized as: p=6 mm, w=1.4 mm, l=3 mm, h=14.7 mm, d=1.2 mm, $Z_S = 5\ \Omega/\square$, the coefficient a in (4) is 0.14.

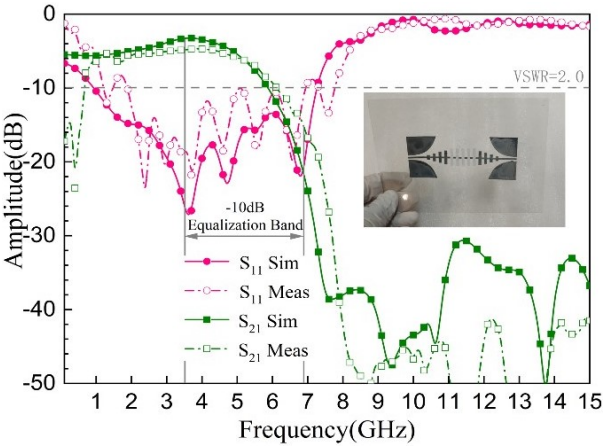

Fig. 6. Measurement and simulation results of the SSPP filter with negative slope equalization.

Before measurement, conductive silver paste is used to bond the SMA connector to the two ports of the filter. The measurement results are obtained by vector network analyzer P5008A of Keysight. It can be seen that the low-pass cut-off frequency of the filter is 8.5 GHz, and negative slope equalization is realized in the passband. The −10 dB equalization band starts at 3.5 GHz (IL = −4.8 dB) and ends at 6.9 GHz (IL = −15.4 dB).

The average reflection coefficient is -13 dB, which is superior to the filter in [13]. The suppression of the upper stopband up to 15 GHz is better than -41 dB, thus the interference can be eliminated effectively. Since the loss of the PET substrate is relatively larger in application compared to theoretical calculation, the insertion loss of the measured curve is greater than the simulated one. However, the advantage of the PET substrate is that it brings the flexibility of the filter in applications, which enables it to be assembled with conformal surfaces and it occupies less volume.

Table 1 compares the performance of the proposed SSPP filter with similar works. It can be observed that the proposed SSPP filter is provided with filtering and negative slope equalization simultaneously, which can compensate for positive fluctuations, such as wideband antenna.

Table 1: Performance comparison with recent reported works

Ref. No.	Function		IL or EV (dB)	FBW	Slope	Struc
	F	E				
[1]	N	Y	9	42%	Positive	SIW
[2]	N	Y	8	50%	Neg.Seg	CPW
[5]	N	Y	8.6	78%	Neg.Seg	Microstrip
[8]	Y	N	1.1	174%	NA	SSPP
[14]	Y	N	1.6	200%	NA	SSPP
This work	**Y**	**Y**	**10**	**65%**	**Negative**	**SSPP**

F=Filter, E=Equalization, N=No, Y=Yes, IL=Insert Loss, EV=Equalizing Value, Struc=Structure, Neg.Seg=Negative Segment, FBW=Fractional Bandwidth

IV. CONCLUSION

In this paper, a SSPP filter with controllable negative slope equalization based on surface resistance of ITO film is designed, fabricated and measured. The dispersion and equalization properties of the SSPP cells are analyzed in detail. Subsequently, a SSPP filter equipped with amplitude equalization is proposed by employing the unit cell, and controlling the cut-off frequency and equalizing value by the width and surface impedance of an ITO strip. Compared with other published works, the verified properties show that the proposed SSPP filter possesses filtering and negative slope equalization properties simultaneously.

ACKNOWLEDGMENT

This work was supported in part by the Natural Science Basic Research Program of Shaanxi Province under Grant 2023-JC-QN-0500, in part by the Scientific Research Program Funded by Education Department of Shaanxi Provincial Government under Grant 23JK0485, 21JK0847, and in part by the National Science Foundation of China under Grant 62301428.

REFERENCES

[1] H. Peng, F. J. Zhao, J. Dong, S. O. Tatu, Y. Liu, N. J. Lin, and T. Yang, "Substrate integrated waveguide equalizers and attenuators with surface resistance," *IEEE Trans. Microw. Theory Techn.*, vol. 68, no. 4, pp. 1487-1495, Apr. 2020.

[2] X. Pang, L. Xia, and J. N. Jiao, "A gain equalizer based on grounded coplanar waveguide with spiral-shaped defected ground," in *2022 IEEE 9th Int. Sym. Microw. Antenna Propag. EMC Technol. Wireless Commun. (MAPE)*, Chengdu, China, pp. 15-19, Aug. 2022.

[3] L. Han, "A reconfigurable microwave equalizer with different maximum attenuations based on RF MEMS switches," *IEEE Sensors J.*, vol. 16, no. 1, pp. 17-18, Jan. 2016.

[4] Y. Itoh and H. Takagi, "L-band SiGe HBT active differential equalizers with variable inclination and position of the positive or negative gain slopes," *46th Eur. Microw. Conf.*, London, UK, Oct. 2016.

[5] T. F. Zhou, Z. G. Wang, W. Huan, and R. M. Xu, "Design of microwave wave gain equalizer using microstrip shorted SIR," in *Int. Conf. Microw. Millim. Wave Technol.*, Shenzhen, China, May 2012.

[6] J. B. Pendry, L. Martín-Moreno, and F. J. Garcia-Vidal, "Mimicking surface plasmons with structured surfaces," *Science*, vol. 305, pp. 847-848, Aug. 2004.

[7] A. P. Hibbins, B. R. Evans, and J. R. Sambles, "Experimental verification of designer surface plasmons," *Science*, vol. 308, pp. 670-672, Apr. 2005.

[8] M. Wang, S. Sun, H. F. Ma, and T. J. Cui, "Supercompact and ultrawideband surface plasmonic bandpass filter," *IEEE Trans. Microw. Theory Techn.*, vol. 68, no. 2, pp. 732-740, Feb. 2020.

[9] J. Wang, K. X. Xu, X. L. Kong, R. F. Xu, and L. Zhao, "Wide-angle beam-scanning leaky-wave antenna array based on hole array SSPPs," *IEEE Antennas Wireless Propag. Lett.*, vol. 22, no. 7, pp. 1731-1735, July 2023.

[10] B. C. Pan, P. Yu, Z. Liao, F. Zhu, and G. Q. Luo, "A compact filtering power divider based on spoof surface plasmon polaritons and substrate integrated waveguide," *IEEE Microw. Wireless Compon. Lett.*, vol. 32, no. 2, pp. 101-104, Feb. 2022.

[11] A. Kianinejad, Z. N. Chen, and C. W. Qiu, "Design and modeling of spoof surface plasmon modes-based microwave slow-wave transmission line," *IEEE Trans. Microw. Theory Techn.*, vol. 63, no. 6, pp. 1817-1825, June 2015.

[12] H. F. Ma, X. P. Shen, Q. Cheng, W. X. Jiang, and T. J. Cui, "Broadband and high-efficiency conversion from guided waves to spoof surface plasmon polaritons," *Laser Photon. Rev.*, vol. 8, no. 1, pp. 146-151, 2014.

[13] C. H. Wang, X. M. Shi, H. L. Yang, and X. L. Xi, "A flexible amplitude equalizing filter based on spoof surface plasmon polaritons," *IEEE Trans. Antennas Propag.*, vol. 71, no. 7, pp. 5777-5785, July 2023.

[14] Y. L. Wu, L. D. Pan, W. M. Wang, Y. H. Yang, Y. W. Wei, H. P. Wu, and L. Ma, "A new self-packaged substrate integrated air-filled spoof surface plasmon polaritons line with inherent low loss and deep upper frequency suppression," *IEEE Trans. Plasma. Sci.*, vol. 48, no. 10, pp. 3516-3523, Oct. 2020.

Chenhao Wang was born in Shaanxi province, China, in 1988. He received the B.S., M.S. and Ph.D. degrees in electromagnetic field and microwave technology from Xi'an University of Technology, Xi'an, China, in 2011, 2014 and 2022, respectively. He currently works at Xi'an Technological University, Xi'an, China. His current research interests include spoof surface plasmon polaritons and novel metamaterial functional devices, including theoretical design and experimental realization.

Junjie Dong received the B.S. degree from China West Normal University, Nanchong, China, in 2021. He is currently pursuing the M.S. degree at Xi'an Technological University, Xi'an, China. His research interests include metamaterial and microwave filters.

Xiaomin Shi received the B.S., M.S. and Ph.D. degrees in electromagnetic field and microwave technology from Xi'an University of Technology, Xi'an, China, in 2006, 2010 and 2017, respectively. She joined the Department of Communication Engineering, Xi'an Shiyou University, in 2017. Her current research interests include microwave circuits and graphene-based devices.

Hailong Yang received the B.S. in communicating engineering from Heze University, Heze, China, in 2012, and M.S and Ph.D. degrees in communicating engineering from Xi'an University of Technology, Xi'an, China, in 2015 and 2019. He joined the faculty of Electronic Engineering Department, Xi'an University of Posts and Telecommunications, in 2019. His research interests include wave propagation and antenna design.